An Intelligent cluster-based segmentation using Wavelet Features:Application to Medical Images

V.Thavavel[a], J. Jaffer Basha[b]

[a]*Department of Computer Applications, Karunya University, Coimbatore, TamilNadu, India*
[b]*Department of Computer Science, Madurai Institute of Engineering and Technology, Madurai, TamilNadu, India*

Abstract

Segmentation forms the onset for image analysis especially for medical images, making any abnormalities in tissues distinctly visible. Possible application includes the detection of tumor boundary in SPECT, MRI or electron MRI (EMRI). Nevertheless, tumors being heterogeneous pose a great problem when automatic segmentation is attempted to accurately detect the region of interest (ROI). Consequently, it is a challenging task to design an automatic segmentation algorithm without the incorporation of *a priori* knowledge of an organ being imaged. To meet this challenge, here we propose an intelligence-based approach integrating evolutionary k-means algorithm within multi-resolution framework for feature segmentation with higher accuracy and lower user interaction cost. The approach provides several advantages. First, spherical coordinate transform (SCT) is applied on original RGB data for the identification of variegated coloring as well as for significant computational overhead reduction. Second the translation invariant property of the discrete wavelet frames (DWF) is exploited to define the features, color and texture using chromaticity of LL band and luminance of LH and HL band respectively. Finally, the genetic algorithm based K-means (GKA), which has the ability to learn intelligently the distribution of different tissue types without any prior knowledge, is adopted to cluster the feature space with optimized cluster centers. Experimental results of proposed algorithm using multi-modality images such as MRI, SPECT, and EMRI are presented and analyzed in terms of error measures to verify its effectiveness and feasibility for medical applications.

Key words: Color image segmentation; Medical image segmentation; Spherical coordinate transform; K-means clustering; Genetic algorithm; Wavelet features; Wavelet frames.

1. Introduction

Accurate delineation of ROI and extraction of quantitative information plays an instrumental role in medical diagnosis and follow-up assessment. Despite numerous efforts by the medical imaging community, accurate and reproducible segmentation of ROIs and characterization of abnormalities still pose challenging and difficult task. The key problem is no single unified segmentation scheme exists to yield acceptable results for different types of medical images. Earlier studies have shown that combining color and texture features would be of significant benefit in distinguishing different classes of pathological tissues [13, 11, 20]. Nonetheless, the effectiveness of texture characterization is bound by the type of algorithm that is used to extract meaningful features. Recently, Multi-scale filtering methods have shown significant potential for texture description, where advantage of the spatial-frequency concept is utilized to maximize the simultaneous localization of energy in both spatial and frequency domains

Email addresses: thavavelmurugesanv@gmail.com (V.Thavavel), jafferbasha@gmail.com (J. Jaffer Basha), rammku@eth.net (R.Murugesan)

[1, 2]. Wavelet transform provides good multi-resolution analytical tool for texture characterization analysis with high accuracy rate. Most of the previous works on wavelet transform have focused on dyadic wavelet transform that are sensitive to translation-variance and may not be desirable in the context of texture characterization [19, 4]. Therefore, the work presented here extracts texture features using discrete wavelet frames [22] to provide a translation-invariant feature description.

Another key problem in clinical medicine is that no complete automatic segmentation exists to free the physician from burden of manual labeling and to provide quantitative measurements to aid in diagnosis. Different complex models of *a priori* information about the expected contents of the image is widely used [21, 23, 3]. The applied *a priori* knowledge consists of a combination of anatomical/physiological information of the image as well as information about the image formation process. The more the contributed model information is verifiable, the more likely is the success of automation of the segmentation process. Unfortunately, the model information is often too complex and/or not exact so that a completely automatic extraction is difficult to realize. To address this issue, the present approach incorporates GKA [9, 15] into the segmentation procedure to learn intelligently the feature image space and identify the optimal cluster centers. The total within cluster square error (TWCSE) forms the basis of an objective function to optimize cluster centers of k-means for successful ROI identification. The feasibility of the proposed approach for medical application is demonstrated with MRI and SPECT images. Also since our interest is towards the enhancement of electron MRI (EMRI), a fast emerging functional imaging modality for noninvasive imaging of free radicals, as a viable technology for biomedical research and clinical applications [6, 7]. The proposed algorithm is evaluated with EMRI of small animals for pharmacokinetic and tumor studies.

2. Color Space Analysis

The advent of functional imaging techniques has opened a wide window for color image analysis. In general, the red-green-blue (RGB) space is used in image processing research, dictated primarily by the availability of such data as they are produced by most color image capturing devices. Drawbacks in the use of RGB in computer vision applications are: the high correlation among RGB channels, the representation of RGB is not very close to the way humans perceive colors and it is not perceptually uniform. The analysis of the pixel color distribution in a color space is not restricted to the RGB space. Indeed, there exists a large number of color spaces which can be used to represent the color of the pixels. But, since the performance of an image segmentation procedure is known to depend on the choice of the color space. Many authors have tried to determine the color spaces which are more appropriate for their specific color image segmentation problems. In this light, SCT have shown good performance in medical applications such as skin lesion identification [10] and in tumor detection [6]. Therefore, the present work, employs SCT on RGB color space of the input image and decouples the brightness information from the color information. The equations relating SCT dimensions to RGB components are given as,

$$L = \sqrt{R^2 + G^2 + B^2} \quad (1)$$

$$a^*(AngleA) = \arccos\left[\frac{B}{L}\right] \quad (2)$$

$$b^*(AngleB) = \arccos\left[\frac{R}{L * \sin(a^*)}\right] \quad (3)$$

3. Wavelet Frames for Feature Extraction

The statistical approaches for feature characterization restrict themselves to the analysis of spatial interactions over relatively small neighborhoods [8]. As a consequence, their performance is good for the class of so-called micro-features. Multi-scale approaches try to overcome the intrinsic limitations of a single-scale analysis of the texture problem. Gabor transforms is widely used to extract feature vectors, which have shown significant potential for texture classification and segmentation [12, 5]. These approaches are supported by experiments on mammalian visual systems, which indicate a reliance of the visual system on spatial-frequency analysis. The potential disadvantage of Gabor filtering is its computational overhead, especially for the evaluation of low-frequency components. In addition, the outputs of Gabor filter banks are not mutually orthogonal, which may result in a significant correlation between features. Most of these problems can be avoided using wavelet transform, which provides a

precise and unifying framework for the analysis and characterization of a signal at different scales.

The wavelet transform downsamples the signal and the length of the decomposed signal is reduced. Therefore the intra-scale and inter-scale fusion schemes for unsupervised texture segmentation, should be taken into account to attain the satisfactory results. In order to overcome this and to obtain more complete characteristic of the analyzed signal, an overcomplete wavelet decomposition is needed in which the output of the filter banks is not subsampled. Unser [22] proposed the overcomplete wavelet representation, DWF by incorporating redundant information to yield a translation-invariant description of texture features. The main advantages of the wavelet frames are that it focuses on scale and orientation texture features and it decomposes the image into orthogonal components. This property yields a better estimation of texture statistics and more detailed characterization at region boundaries. DWF decompositions are calculated by successive 1D processing along the rows and columns of the image with two-scale relation defined as,

$$h_{i+1}(k) = [h]_{\uparrow 2^i} * h_i(k) \quad (4)$$

$$g_{i+1}(k) = [g]_{\uparrow 2^i} * h_i(k) \quad (5)$$

where notation $[.]_{\uparrow m}$ denotes the upsampling by a factor of m. The factor of one iteration is more or less to dilate the filters h_i and g_i. Each step involves a convolution with the basic filters h and g, which are expanded by inserting appropriate number of zeros between taps. The complexity of this algorithm is same to all iterations and proportional to the number of samples.

$$s_{i+1}(k) = [h]_{\uparrow 2^i} * s_i(k) \quad (6)$$

$$d_{i+1}(k) = [g]_{\uparrow 2^i} * s_i(k) \quad (7)$$

3.1. Color Feature Extraction

Most of the existing color extraction techniques are based on the color image histogram [16, 17]. Even though such techniques have been quite successful in given settings, they have notable shortcomings. First, the histogram does not incorporate any spatial information. Second, the color histogram is too finely quantized in color space, and hence does not take into consideration the fact that the human visual system can only perceive a few colors at a time. To combat these problems, Ma et al [18] were the first to propose a compact color representation in terms of dominant colors for image segmentation and retrieval. There are number of approaches for extracting the dominant colors. One such approach is to apply low-pass filtering on the original image to obtain the average color within the squared window as well to eliminate the spurious pixels within uniform regions. To this fact, the work presented here adopts DWF to obtain the similar result with less computational complexity and uses the chromaticity channels (a, b) of LL band to define the color features as follows,

$$chroma = \sqrt{a^2 + b^2} \quad (8)$$

3.2. Texture Feature Extraction

Texture is the discriminating information that differentiates normal from abnormal lesions. Since texture is essentially a multi-scale phenomenon, multi-resolution approaches perform well for texture analysis. A characterization of texture is usually based on the local information that appears within a neighborhood distribution. Recent studies have come to the conclusion that a spatial/frequency representation, which preserves both global and local information, is adequate for the characterization of texture. Since wavelet transform offers a tool for spatial/frequency representation, wavelet frame representation of wavelet transform are employed for spatial texture feature extraction [14, 22, 17]. Such representations is also proposed in the present study because they are more robust, sparse, and can have greater flexibility in representing the structure of the input data.

The most commonly used features for texture analysis in the context of multi-scale frequency decompositions is the energy of the subband coefficients [17]. The coefficients are quite sparse. Therefore, it is necessary to perform some type of window operation to obtain a more uniform characterization of texture. Here, we use local median energy, where the energy is defined as the square of the coefficients as given in Eqn. 9.

$$energy = \frac{1}{M}\Sigma_{m=1}^{M}\Sigma_{n=1}^{M}|x(m,n)|^2 \quad (9)$$

The advantage of using median filter is that it preserves the energy associated with texture between regions. Further the low-frequency image produced by the wavelet transform does not contain major texture information,

and the most significant information of a texture often appears in the middle-frequency channels. Considering these facts, the present work extracts texture features using the luminance channel of the coefficients in LH and HL decompositions. Finally feature vector generated for every pixel in the image is 3-dimensional that includes color value (chroma) and texture information in the form energy values in LH and HL subbands (E_{lh}, E_{hl}).

4. Genetic K-Means Clustering

Clustering has been effectively applied in a variety of engineering and scientific disciplines. Cluster analysis organizes data (pattern) by abstracting underlying structure. The grouping is done such that patterns within a group (cluster) are more similar to each other than patterns belonging to different groups. Thus, organization of data using cluster analysis employs some dissimilarity measure among the set of patterns. The dissimilarity measure is defined based on the data under analysis and the purpose of the analysis. Various types of clustering algorithms have been proposed to suit different requirements and are broadly classified into hierarchical and partitional algorithms based on the structure of abstraction [24, 9]. Hierarchical clustering algorithms construct a hierarchy of partitions, represented as a dendrogram in which each partition is nested within the partition at the next level in the hierarchy. Partitional clustering algorithms generate a single partition, with a specified or estimated number of non overlapping clusters, of the data in an attempt to recover natural groups present in the data. The simplest and most popular partitional clustering algorithm is the K-means algorithm (KMA). KMA is an appropriate tool under the assumption that the clusters are hyperspheroidal since distance measures are employed. However, real data sets seldom approach this hyperspheroidal idealization and the algorithm may converge to a suboptimal partition with random initialization of centroids. The basic idea of applying GA to clustering is to simulate the evolution process in nature and evolve clustering solutions from one generation to the next. In contrast to the KMA, which might converge to a local optimum, the genetic clustering algorithm is insensitive to the initial assignment and mostly converges to the global optimum eventually [15]. Hence this work attempts to apply the GKA to cluster the feature vector of the medical image data, with the expectation of global optimal clustering solution with higher detection accuracy.

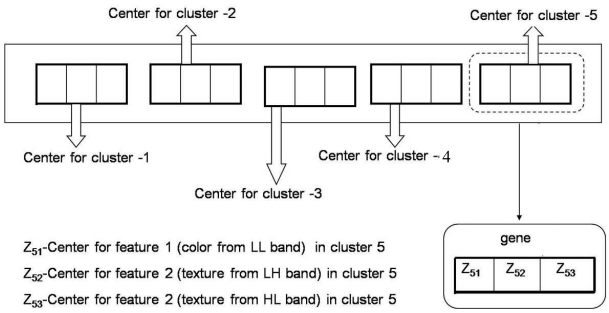

Figure 1: Chromosome Encoding for GA-based Wavelet Segmentation

4.1. Chromosome Encoding

Fundamental to all GA's is the encoding scheme for representing the solutions of the corresponding optimization problems. Normally, the method used to encode the solutions depends not only on the problem to which the GA is applied but also on the genetic operations used. In the present study, the numerical feature values of all cluster centers are encoded into a real-coded chromosome. Each chromosome represents a clustering solution consisting of centers for the given number of K clusters. An example of chromosome representation is depicted in Fig. 1, in which the clustering solution has 5 cluster centers with feature vector of three values. Each feature value is randomly initialized and limited within lower and upper boundary of its possible values. For large and high-dimensional data, this encoding is more scalable than the encoding using the number of data patterns.

4.2. Fitness Function

The global searching ability of GA is utilized in the present work to appropriately determine a fixed number K of cluster centers in 2D Euclidean space. The TWCSE, adopted as a clustering metric is defined as the sum of the Euclidean distances of the pixels from their respective cluster centers and can be given as follow for K clusters $C_l, C_2, C_3, \cdots, C_k$,

$$TWCSE(\delta) \quad = \quad \Sigma_{k=1}^{k} \Sigma_{X_i \varepsilon C_k} \|X_i - Z_k\|^2$$

Table 1: Optimization parameters for GA-based Wavelet Segmentation

Genetic operator	Optimization Parameter
Initial Population	100 Chromosomes
Encoding	Real Coded String
Fitness Function	Minimize TCWSE
Selection	Roulette Wheel Selection
Crossover	K-point crossover with probability of 0.8
Mutation	Three-point mutation with probability of 0.6

$$Z_k = \frac{\Sigma_{X_i \varepsilon C_k} X_i}{|C_k|} \quad (10)$$

where $|C_k|$ denotes the number of pixels in C_k, $(Z_1, Z_2, Z_3, \cdots, Z_k)$ denotes the target cluster centers. In this context, the objective of the proposed algorithm is to find K optimal cluster centers to partition the N patterns into user-defined K groups, such that this partition minimizes the total within cluster square error (TWCSE) defined as

$$Objective function(\delta) = min(TWCSE(\delta)) \quad (11)$$

4.3. Crossover and Mutation

In the present study, 100 individual solutions (chromosomes) were selected for reproduction after intensive experiments. The probability of selecting a particular solution increases with its fitness value, defined by Eqn. 11. The cluster centers of the selected solutions are perturbed to reduce the possibility of trapping in local optima. New chromosomes are generated from these perturbed chromosomes using crossover and mutation of genes. In crossover, solutions (chromosomes) are paired according to their similarity in fitness and within each solution pair, the cluster centers are paired based on their closeness in Euclidean distance. Then, a segment of one of the three genes (either of the feature) of a cluster center is swapped with the corresponding gene segment from the paired cluster center. The same procedure is done for all paired cluster centers. In genetic terms, this is called K-point crossover. Mutation is achieved by perturbing each of the three feature gene values within the allowed range with high mutation rate of 0.6.

4.4. Convergence

The goal of employing a GA for optimizing cluster centers of k-means is to converge on a global optimal solution for each feature through the possible genes for which the TCWSE is minimized. The convergence criterion is thus the minimum TCWSE, but since it is not known *a priori*, it cannot be used to test whether the algorithm has converged. Hence the common practice is to terminate the GA after a pre-specified number of generations, and then test the quality of the best members of the population against the problem definition. In the present work the maximum number of generations of 150. The genetic parameters that were found to give optimal performance are listed in Table 1.

Table 2: Pseudocode of GA-based Wavelet Segmentation

```
1.  Apply DWF on image
2.  Define 3D feature vector for each image pixel by
    extracting the color feature from LL subband and texture
    feature from HL and LH subband
3.  Initialize genetic parameter and population with randomly
    generated cluster centers
4.  While ((TWCSE is not optimized) {
    for i = 1 to popSize do
    Calculate the fitness value using Eqn (11)
    Calculate the selection probability
    Select parents and
    Apply crossover & create offspring
    Mutate offspring
    end for
    Replace the old population by the new one }
5.  Cluster the feature space using the GA optimized centers
6.  Find the edge map for the clustered image and superimpose
    on the original image to determine the accuracy of the
    proposed system
```

5. Results and Discussion

The potency of the proposed algorithm which is tabulated in Table 2 was first investigated with functional MRI data to determine its accuracy for brain tumor segmentation, as they are not discriminative enough when the appearance of tumor and normal tissue overlap. The promising results on fMRI encouraged the application of the proposed algorithm for SPECT and *in vivo* EMR images. In all these experiments, 9/7 biorthogonal wavelet decomposition with the energy median in a window of size 9x9 were employed for feature characterization. Also, certain colors were used to represent significant features in EMR

images. For example, the spin probe distribution is normally mapped to red in color.

5.1. Application to fMRI

This section evaluates the performance of the proposed system for brain tumor segmentation on fMRI data. The reference fMRI with metastatic brain tumor depicted in column (A) of Fig. 2 was obtained from the open source database. The image was collected using a 1.5 Tesla Siemens Vision MRI scanner (Siemens AG, Erlangen, Germany) while the patient was subjected to the task of information storage and retrieval, thought, emotions, and initiation of behavior. A total of 256 EPI volumes were acquired using a T2 weighted gradient single-shot EPI sequence with TR = 1648ms, TE = 45ms, Flip Angle = 90 and FOV = 250 x 250 mm2. Each volume covered the tumor and potential surgical corridors, consisting of 15 transverse slices of size 64 x 64 with a pixel size of approximately 3.91 x 3.91 mm2 and a slice thickness of 6 mm with no gaps.

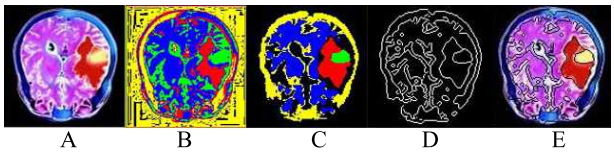

Figure 2: Application to MR images for tumor studies

From visual inspection of Fig. 2, it is interesting to notice that the proposed method produces better segmentation results than the standard Kmeans-based method by obviously discriminating the tumor and normal brain area without using prior knowledge of anatomical structures. On other hand, the inefficiency of the standard approach can be evidenced by the misclassification of healthy tissues as tumor region (shown in green). These advantages of the proposed system are due to fact that the selection of cluster centers is based on the optimization of TWCSE. These results enabled the application of the proposed GKA-based algorithm for SPECT brain perfusion images to assess the cerebrovascular reserve and are described in next section.

5.2. Application to SPECT images

This section assesses the performance of the proposed system with images from brain perfusion SPECT to spot out the region with prominent, normal and decreased activity. The set of axial images of cerebral perfusion used for evaluation were collected from Dartmouth-Hitchcock medical center website [63] and are shown in column (A) of Fig 3. The reference test images had been acquired from a patient with left sided cerebrovascular accident (CVA) after the intravenous administration of acetazolamide (Diamox) using Tc-99m ECD. For sake of comparison, the performance of Kmeans-based segmentation (column B) is depicted along with the response of the proposed GA-based Kmeans segmentation (column C) in Fig. 3. In these results the more prominent, normal and decreased region of brain perfusion is depicted in red, green and blue color respectively. Also, the result of binarization of edge map obtained by applying canny operator on the segmented image (column C) is given in column D. The column E shows the results of superimposing the contours (column C) over the corresponding reference input image (column A). From visual inspec-

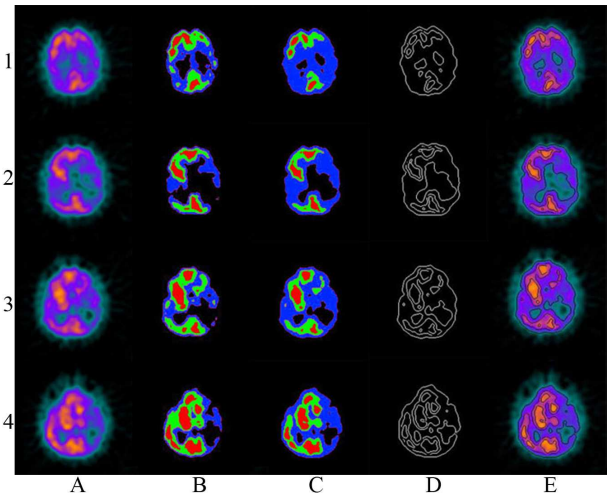

Figure 3: Application to SPECT brain perfusion images

tion of Fig. 3, it is interesting to notice that the proposed method accurately discriminates the decreased perfusion region to the left cortical hemisphere, including frontal, parietal, temporal and occipital regions. Also it clearly marks out the area of severe hypoperfusion in the right parietal and superior temporal regions (reflects infracted tissue). On other hand, the broad area of decreased perfusion shown in blue color in column B shows the limita-

tion of the Kmeans-based approach. The advantage of the proposed system is due to fact that the selection of cluster centers is based on the optimization of TWCSE. Based on these encouraging results application of the GA-based Kmeans algorithm for feature identification in EMR tomograms is described in the next section.

5.3. Application to EMRI

One of the principal objectives of the development of the proposed system was to study the time profile of uptake and clearance of EMR imaging agents in mice tumor models. Hence the integrated ROI identification system was evaluated for its performance using in vivo murine EMR images. Two different sets of images were used for the validation. The first set consisting of a sequence of temporal images depicting the renal clearance of the imaging agent OXo63 and the other showing the uptake and clearance of the imaging agent AMCPy in RIF tumor present in one of the legs of a mouse. The details of whole body and tumor imaging experiments are described in [6, 7].

5.3.1. Renal Imaging

The input EMR images used to evaluate the performance of the proposed ROI identification system are shown in column A of Fig. 4. These images show the progressive accumulation of the spin probe in left and right kidneys and the bladder of a C3H mouse after the injection of Oxo63 solution at 2.8, 9.0, and 18.0 min, respectively. The results of the proposed algorithm for EMR renal images are presented in Fig. 4 and aligned as in Fig. 3. It can be readily seen from Fig. 4 that the proposed method taking the advantage of the feature values, texture and color, is able to process the intensities of spin probe distribution in various mouse organs with the recognized optimal centers of GKA-based algorithm. On contrary, the inability of standard k-means to accurately reveal the spin probe distribution can be noticed especially when comparing red and green labels in column B. This is due to the fact that standard k-means is sensitive to selection of initial partitions and converges to a local minimum of the criterion function value. Having identified that the optimal segmentation results correspond to the images given in column C, we proceed to use these images to derive the kinetics of clearance of the imaging agents from the three

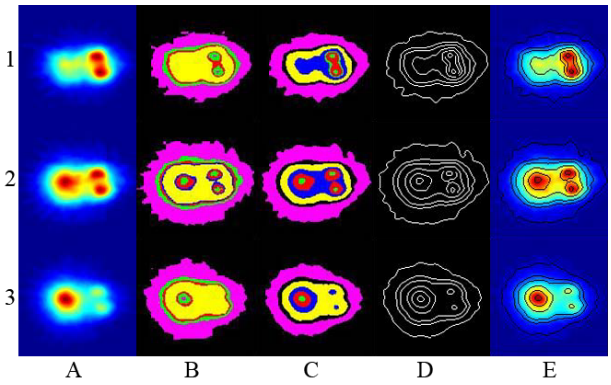

Figure 4: Application to EMR images for pharmacokinetic studies

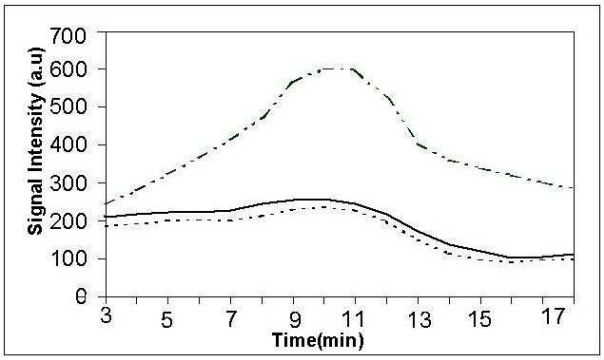

Figure 5: Visualization of the clearance of imaging agent as evaluated from ROI identified by the proposed system

ROIs identified, viz: the left and right kidneys and the bladder. Visualization of the renal clearance of the imaging agent is depicted in Fig. 5. The signal intensity corresponds to the average pixel count computed from the three ROIs, left kidney (A), right kidney (B) and the bladder (C). The signal intensity corresponds to the average pixel count computed from the three ROIs, left kidney (——), right kidney (. . . . .), and bladder (– · · – ··) .

5.3.2. Uptake and Clearance of Imaging Agent in Tumor

One of the major aims of the present system is to facilitate the recognition of features of interest in EMR tomograms. Because of its capability to measure the pO2 and redox status in tumor of animal models, EMRI is fast becoming a functional imaging modality in cancer research. However, segmentation of tumor in EMR tomograms is

a difficult task, because the intensity levels vary greatly across different regions due to the heterogeneity in tumors.

In order to examine the tumor identification by the proposed algorithm, EMR image of a mouse with RIF tumor in its right hind leg was considered as the input image and results are summarized in Fig. 6. These images show the distribution of spin probe AMCPy in the normal and tumor legs of the mouse at 1, 5, and 15 min after the infusion of the spin probe by tail-vein cannulation. The description of rows and columns is the same as that for Fig.2.

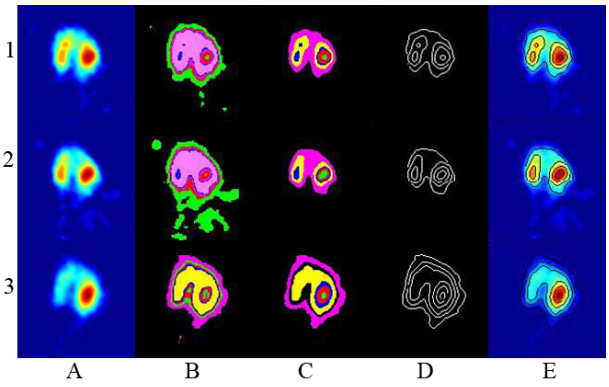

Figure 6: Application to EMR images for tumor studies

From Fig. 6, it can be observed that the proposed approach which employs the color and texture features extracted from wavelet framework has resulted in better segmentation of the tumor (Fig. 6(C)). Further it can be evidenced that the proposed method is able to vividly discriminate the imaging agent distribution in tumor bearing right hind leg and the normal leg. This clearly demonstrates the advantages of the proposed approach, which adopts GA to intelligently determine the optimal cluster centers for each area of the image and then segment the image accordingly. Alternatively, it can be noticed from red and green labels in Fig. 6(B) that the standard approach is incapable to distinguish various regions of the image that leads to significant misclassification and meaningless results

5.4. Quality Measures

Accurate segmentation plays an important role in medical image processing, because an error in this process can lead to an error in diagnostic as well as treatment processes. Hence the performance of the proposed algorithm is also evaluated quantitatively using the common TWCSE measurement. The error factor was computed using Eqn. 10. The error measurement computed for all the above experiments are collected in Table. 3.

Table 3: Error measures for SPECT images

Brain MRI (in Fig 2)	Error Value	
	Kmeans-based ROI (in Column B)	GKA-based ROI (in Column C)
Row 1	13.2	0.33
Brain SPECT (in Fig. 3)	Kmeans-based ROI (in Column B)	GKA-based ROI (in Column C)
Row 1	5.2	0.14
Row 2	4.7	0.12
Row 3	3.3	0.13
Row 4	2.6	0.12
Renal EMRI (in Fig. 4)	Kmeans-based ROI (in Column B)	GKA-based ROI (in Column C)
Row 1	3.4	0.21
Row 2	7.1	0.16
Row 3	11.2	0.13
Tumor EMRI (in Fig. 6)	Kmeans-based ROI (in Column B)	GKA-based ROI (in Column C)
Row 1	7.3	0.16
Row 2	11.8	0.12
Row 3	4.2	0.11

Thus from visual and quantitative evaluations, it can be inferred that GKA-based approach performs intelligently well in accurately identifying the ROI for all kinds of functional medical images. Nonetheless, the GKA-based method may have less advantage in terms of computational overhead when compared to the conventional Kmeans-based method. However, this may not be a serious problem, because in many applications the medical image segmentation is an off-line process. But, this may pose problem when real time dynamic imaging is performed. Under such circumstances, this problem may be addressed by taking advantage of the parallel computing nature of GA.

6. Conclusion

This paper presents an intelligence-based scheme for ROI identification incorporating GA and Kmeans within the multi-resolution framework. The proposed approach provides a pathway for concise and precise identification of ROI in medical image without *a priori* knowledge of the anatomic structure of interest. The feasibility of the proposed scheme was tested with functional medical images for tumor and pharmacokinetic studies. Results demonstrated the potency of the system in accurately identifying the pathological tissues with fMRI and regions of severe hypoperfusion with SPECT perfusion brain images. Encouraging results, motivated to evaluate the new approach for newly evolving modality, EMRI. With renal imaging, the approach accurately outlined the spin density distribution in bladder and kidney. In murine tumor imaging, the proposed approach reveals its capability in marking out the differences in perfusion of the imaging agent between the normal and tumor legs.

References

[1] K. W. Abyoto, S. J. Wirdjosoedirdjo, and T. Watanabe. Unsupervised texture segmentation using multiresolution analysis for feature extraction. *J. Tokyo Univ. Inform. Sci.*, 2:49–61, 1998.

[2] G. Boccignonea, P. Napoletano, V. Caggiano, and M. Ferraro. A multiresolution diffused expectation-maximization algorithm for medical image segmentation. *Computers in Biology and Medicine*, 37:83–96, 2007.

[3] O. Colliot, O. Camara, and I. Bloch. Integration of fuzzy spatial relations in deformable modelsapplication to brain mri segmentation. *Pattern Recognition*, 39:1401–1414, 2006.

[4] G. Van deWouwer, P. Scheunders, S. Livens, and D. Van Dyck. Wavelet correlation signatures for color texture characterization. *Pattern Recognition*, 32:443–451, 1999.

[5] D. Dun, W. Higgins, and J. Wakeley. Texture segmentation using 2-D gabor elementary functions. *IEEE Trans. Patt. Anal. Mach. Intell.*, 16:130–149, 1994.

[6] D. C. Durairaj, M. C. Krishna, and R. Murugesan. Integration of color and boundary information for improved region of interest identification in electron magnetic resonance images. *Computerized Med Imaging and Graphics*, 28:445–452, 2004.

[7] D. C. Durairaj, M. C. Krishna, and R. Murugesan. A neural network approach for image reconstruction in electron magnetic resonance tomography. *Comput. Biol. Med.*, 37:1492–1501, 2007.

[8] L. Ganesan and P. Bhattacharyya. A new statistical approach for micro texture description. *Pattern Recognition Letters*, 16:471–478, 1995.

[9] O. Hall, I. Barak, and J. C. Bezdek. Clustering with a genetically optimized approach. *IEEE Trans. Evo. Comput.*, 3:103–112, 1999.

[10] G. A. Hance, S. E. Umbaugh, R. H. Moss, and W. V. Stoeckers. Unsupervised color image segmentation with application to skin tumor borders. *IEEE Eng. Med. Biol*, 15:104–111, 1996.

[11] H. Handels and T. Ross. Feature selection for optimized skin tumor recognition using genetic algorithms. *Artificial Intelligence in Medicine*, 16:283–297, 1999.

[12] A. K. Jain and F. Farrokhnia. Unsupervised texture segmentation using gabor filters. *Pattern Recognition*, 24:1167–1186, 1991.

[13] S. A. Karkanis, D. K. Iakovidis, D. E. Maroulis, D. A. Karras, and M. Tzivras. Computer-aided tumor detection in endoscopic video using color wavelet features. *IEEE Trans. Inf. Technol. Biomed.*, 7:141–152, 2003.

[14] S. C. Kim and T. J. Kang. Texture classification and segmentation using wavelet packet frame and gaussian mixture model. *Pattern Recognition*, 40:1207–1221, 2007.

[15] K. Krishna and M. N. Murty. Genetic k-means algorithm. *IEEE Trans. on Systems, Man, and Cybernetics - Part B: Cybernetics*, 29:433–439, 1999.

[16] N. Lian, V. Zagorodnov, and Y. Tan. Color image denoising using wavelets and minimum cut analysis. *IEEE Signal Processing Letter*, 12:741–744, 2005.

[17] S. Liapis and G. Tziritas. Color and texture image retrieval using chromaticity histograms and wavelet frames. *IEEE Trans. on Multimedia*, 6:676–686, 2004.

[18] W. Y. Ma, Y. Deng, and B. S. Manjunath. Tools for texture/color based search of images. *Human Vision and Electronic Imaging II,Proc. SPIE*, 3016:496–507, 1997.

[19] A. Sengur. Wavelet transform and adaptive neuro-fuzzy inference system for color texture classification. *Expert Systems with Applications*, 34:2120–2128, 2008.

[20] A. B. Tosuna, M. Kandemira, C. Sokmensuerb, and C. Gunduz-Demira. Object-oriented texture analysis for the unsupervised segmentation of biopsy images for cancer detection. *Pattern Recognition*, 42:1104–1112, 2009.

[21] A. Tsai, A. Yezzi, W. Wells, C. Tempany, D. Tucker, A. Fan, W. E. Grimson, and A. Willsky. A shape-based approach to the segmentation of medical imagery using level sets. *IEEE Trans. Med. Imag.*, 22:137–154, 2003.

[22] M. Unser. Texture classification and segmentation using wavelet frames. *IEEE Trans. Image Process.*, 4:1549–1560, 1995.

[23] Wang and W. G. Wee. Deformable contour method: A constrained optimization approach. *Int. J. Comput. Vision*, 59:87–108, 2004.

[24] R. Xu and D. Wunsch. Survey of clustering algorithms. *IEEE Trans. on Neural Networks*, 16:645–678, 2005.